Calculated rotational spectrum of Ar···CO from an *ab initio* potential energy surface: A very floppy van der Waals molecule

Victoria Castells
LURE[a] *and Laboratoire de Photophysique Moléculaire,*[b] *Université Paris-Sud, 91405 Orsay, France*

Nadine Halberstadt
Laboratoire de Photophysique Moléculaire,[b] *Université Paris-Sud, 91405 Orsay, France*

Seung Koo Shin
Department of Chemistry, University of California, Santa Barbara, California 93106-9510

Robert A. Beaudet and Curt Wittig
Department of Chemistry, University of Southern California, Los Angeles, California 90089-0482

(Received 12 November 1993; accepted 16 March 1994)

Using the *ab initio* potential of Shin *et al.* (to be published), we have calculated the bound states and infrared absorption spectrum of the van der Waals complex Ar···CO. The results show that Ar···CO cannot be treated as a quasirigid rotor, nor as a molecule with a free internal rotor. In particular, a transition to the first excited van der Waals bending level is predicted to be present in the spectrum, and its frequency varies with Ω (the projection quantum number of the total angular momentum onto the intermolecular axis going from the center of mass of CO to the Ar atom). It is also shown that, although the spectrum cannot be analyzed by the use of a rigid rotor model, rotational "constants" can still be defined for each value of Ω. This is consistent with the available experimental data and the predicted bending excitation can account for unassigned transitions in the infrared spectrum of this complex. Finally, a sensitivity analysis of the calculated spectrum with respect to the potential anisotropy has been performed.

I. INTRODUCTION

Studies of van der Waals and hydrogen bonded complexes are very important to understand the weak, intermolecular forces present between atoms and molecules. During the past few decades, these species have been the focus of intense experimental and theoretical studies.[1–7] A variety of dynamical phenomena have been investigated, such as rotational and vibrational predissociation, IVR, cage effect, electronic predissociation, and even chemical reactivity.

The van der Waals complexes built with a diatomic molecule and a rare gas atom are of particular interest, since they represent the simplest case in which anisotropic intermolecular forces can be important. The intermolecular dynamical properties of this type of complexes range from those of a nearly free internal rotor (such as H_2 in the H_2···Ar dimer[8]) to those of an anharmonic oscillator/rigid rotor molecule [like I_2···Ar (Ref. 9) or the rare gas···Cl_2 complexes[10–13]]. A very interesting intermediate case is constituted by complexes of the type of Rg···HX, where Rg is Ne, Ar, Kr, or Xe, and X is F or Cl. In this case, the amplitudes of the van der Waals bending vibrations are very large due to the small mass of the hydrogen atom. Also, these complexes have usually two minima which are both collinear, Rg···HX or Rg···XH.[14] The calculation of vibration-rotation spectra by Clary and Nesbitt[15] for Rg···HCl predicted surprisingly large intensities for transitions to states with multiple vibrations excited in the bending mode.

The complexes of CO with a rare gas atom (He, Ne, Ar) or H_2 also lie between the semirigid and nearly-free internal rotor limits,[16] making the assignment of the spectrum more difficult. The Ar···CO dimer is one of the simplest atom–diatom van der Waals complexes consisting entirely of heavy species, which could also possess unusually large amplitude bending vibrations. Several intermolecular potential energy surfaces have been proposed to date. The first one was designed by Parker and Pack[17] using the electron gas model, for studies of rotationally and vibrationally inelastic collisions of Ar with CO. Semiempirical dispersion coefficients C_6 and C_8 were determined, and two resulting potentials were obtained. Both reproduced the second virial coefficients very well. The well depth of the first potential was nearly the same at all angles, with a maximum depth of 103 cm^{-1} at $R=3.77$ Å and $\theta=102°$ (see the definition of these coordinates in Fig. 1). The well depth of the second potential varied more with angle and had a maximum depth of 141 cm^{-1} at 3.57 Å and $\theta=85°$. A year later, Mirsky[18] evaluated the CO···Ar interaction potential in order to investigate the properties of the solid CO–Ar system. The potential was expressed as a sum of the C···Ar and O···Ar interatomic interactions, which were derived from the C···C, O···O, and Ar···Ar exponential-6 potentials using combining rules. The equilibrium position for the Ar atom is at 3.63 Å from the center of mass of CO, with $\theta=77°$ and the depth of the potential well equal to 110.4 cm^{-1}. The potential well was also found to be shallow along the minimum energy path going from the equilibrium position to the oxygen end, the barrier at the oxygen end being 23 cm^{-1} (the barrier to go around the carbon end being slightly higher, 45 cm^{-1}). More recently, Parish *et al.* have explored the difference between oxygen-end and carbon-end bonding in a variety of CO com-

[a]Laboratoire CNRS, MEN et CEA.
[b]Laboratoire propre du CNRS.

 0021-9606/94/101(2)/1006/13/$6.00 © 1994 American Institute of Physics

Downloaded 19 Aug 2003 to 128.125.187.57. Redistribution subject to AIP license or copyright, see http://ojps.aip.org/jcpo/jcpcr.jsp

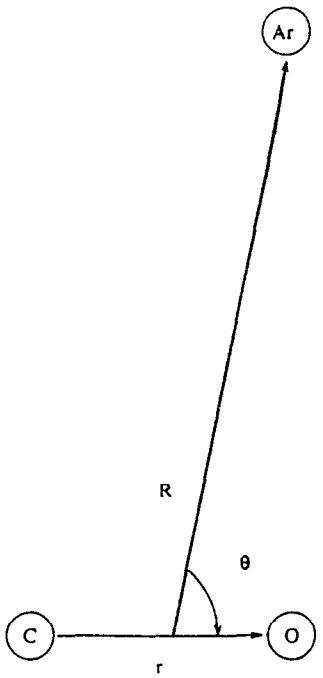

FIG. 1. Coordinate system for the Ar···CO complex.

plexes using the molecular mechanics for clusters (MMC) computational method.[19] This MMC potential is obtained by combining intermolecular electrical interactions with empirical 6-12 potentials. The equilibrium configuration is at $R=3.814$ Å and $\theta=49°$, with $D_e=158$ cm^{-1}. Finally, Shin *et al.*[20] have carried out an *ab initio* calculation for the Ar···CO interaction. The potential well depth corrected for the basis set superposition error is 69 cm^{-1}, with $R_e=4.0$ Å and $\theta_e=100°$ at the MP2 level. The barrier to the oxygen-end configuration is 8 cm^{-1} and that to the carbon-end configuration is 25 cm^{-1}.

In recent years, tremendous progress has been made in the experimental study of weakly bound complexes by employing various high-resolution spectroscopic techniques such as Fourier transform-microwave, diode laser infrared, and laser-induced fluorescence spectroscopy. Such high resolution spectra provide the most precise means to probe intermolecular forces and intermolecular dynamics. Although Ar···CO is one of the simplest van der Waals complexes, the first glimpse of the Ar–CO infrared spectrum in the region of the $v_{CO}=1\leftarrow0$ transition was reported only recently by De Piante *et al.*[21] This was followed by extensive measurements and analyses of the infrared spectrum of Ar···CO by McKellar and co-workers,[22] who combined results from two complementary techniques. The first one involved a pulsed slit-supersonic expansion together with a tunable diode laser similar to the apparatus employed by De Piante *et al.*,[21] and had the advantage of very low (≃10 K) temperature and narrow linewidth (≃0.0003 cm^{-1}). The second one involved a Fourier transform spectrometer and a long-path low-temperature absorption cell. Although it suffered from greater linewidth (≃0.007 cm^{-1}) and interference from monomer absorption, the higher temperature (≃60 K) and wide coverage were complementary to the laser/jet spectra and helped to extend the analysis to higher J-values. As expected in the case of an atom–diatom complex with the atom relatively heavy compared to the diatom and the atom–diatom distance larger than the diatom bond length,[9] the Ar···CO spectrum behaves approximately as a T-shaped near-prolate asymmetric rotor, with K_a as a good quantum number. However, it could not be fitted with an asymmetric rotor Hamiltonian and the analysis was performed by adopting a near symmetric rotor energy level expression including centrifugal distortion constants, but no A constant; the origins of each stack of levels denoted by $K=0$, 1, 2, and 3 were additional parameters in the analysis. Also, a number of lines could not be accounted for. It was proposed[22] that they could involve excited bending states of the complex.

Recently, Ogata *et al.*[23] have measured the microwave rotational spectrum of the Ar···CO complex for different isotopic variations of CO. The results confirm that the complex is a prolate near-symmetric rotor with essentially T-shaped structure, and that it undergoes large amplitude zero-point motion. Three different methods were used to determine an effective value for the angle θ and they gave three different geometrical parameters. It is also shown that the argon is on average closer to the oxygen than to the carbon.

Finally, Havenith *et al.*[24] have just reported measurements of the first excited bending state of Ar···CO in the infrared (IR) region, using a computer-controlled diode laser spectrometer and a continuous slit nozzle supersonic expansion. Effective modulation of van der Waals cluster concentration was achieved by dissociating the weakly bound clusters with each half-cycle of an ac discharge at 5 kHz, allowing detection by a lock-in amplifier. A better signal to noise ratio was obtained by combining the concentration modulation with frequency modulation. Using this technique, they could observe the transition from the ground state, $v_{CO}=0$, $K=0$, to the $v_{CO}=1$, $K=0$, first excited bending state of Ar···CO. No Q branch could be observed. From these results, they found that the first excited $K=0$ bending state of Ar···CO lies at 11.914 cm^{-1} above the $K=0$ ground state.

The only detailed theoretical calculations on the bound energy levels of Ar···CO to have been published are those of Tennyson *et al.*,[25] who used the potential energy surface of Mirsky.[18] In their work, both classical and exact quantum mechanical calculations were performed, and attention was directed at the onset of irregular behavior in the structure of the rovibrational energy levels. Although useful for understanding the general pattern of the Ar···CO levels, they were not complete enough to be directly applied in analyzing the observed spectra.

The purpose of this paper is to show that the inadequacy of the rigid rotor model to the Ar···CO spectrum comes from the strong delocalization of the wave function. This is quite unusual for a complex not involving a very light atom. We have calculated the infrared spectrum of Ar···CO using the most recent *ab initio* potential calculated by Shin *et al.* The results presented here will also provide a test of the quality of this potential and the validity of the full counterpoise

Downloaded 19 Aug 2003 to 128.125.187.57. Redistribution subject to AIP license or copyright, see http://ojps.aip.org/jcpo/jcpcr.jsp

method for the basis set superposition error correction. We compare the theoretical rotational spectrum with the experiment of McKellar *et al.*[22] We determine the averaged structure for the ground vibrational state and compare with the results derived from the microwave experiment of Ogata *et al.*[23] We also predict the bending excitation frequency, which should be observable in the infrared absorption spectrum. We show that it depends on the value of Ω, the projection quantum number of the total angular momentum onto the intermolecular axis (going from the center of mass of CO to the Ar atom). We compare the energy of the first excited bending level with the one deduced by Havenith *et al.*[24] Finally, we study the sensitivity of the results on the anisotropy of the potential.

The main characteristics of the *ab initio* potential are briefly presented in Sec. II. The method used for calculating the Ar···CO bound states and infrared absorption spectrum is described in Sec. III, as well as the two limiting cases against which it could be confronted, the rigid rotor molecule and the free CO internal rotor. Section IV gives the results and their discussion and Sec. V is devoted to conclusions.

II. *AB INITIO* POTENTIAL

The *ab initio* Ar···CO interaction potential was calculated using Møller–Plesset second-order perturbation (MP2) methods by Shin *et al.*[20] The potential surface grid was obtained for eleven values of the intermolecular distance R_i ($\mathbf{R}$ is the vector from the center of mass of CO to the Ar atom), and 19 values of θ_k (θ_k is the angle between $\mathbf{R}$ and the CO axis) equally spaced between 0 and π. The coordinates are illustrated in Fig. 1. The CO bond distance was fixed at its equilibrium value of 1.1281 Å. Thus, the vibration of CO was kept frozen.

Standard double-ζ basis sets for carbon $(9s5p/3s2p)$ and oxygen $(9s5p/3s2p)$ and McLean and Chandlers contracted basis sets for argon $(12s8p/5s3p)$ were used with one set of d-polarization functions for carbon and oxygen $[\zeta(\mathrm{C})=0.70,\ \zeta(\mathrm{O})=1.11]$ optimized for CO at the Hartree Fock level and for argon ($\zeta=0.40$) optimized for Ar at the Hartree Fock level. In addition, these basis sets were augmented with one set of diffuse d-functions $[\zeta(\mathrm{C})=0.70,\ \zeta(\mathrm{O})=1.11,\ \zeta(\mathrm{Ar})=0.40]$. Each point on the potential grid was corrected for the basis set-superposition error by using the full counterpoise method. The points are given in Ref. 20, and the corresponding equipotentials are drawn in Fig. 2(a).

These points were used to determine the coefficients of the expansion of the potential on Legendre polynomials at each value R_i of the grid in the intermolecular distance

$$V_{\mathrm{Ar}\cdots\mathrm{CO}}(R_i,\theta_k)=\sum_{\lambda} v_\lambda(R_i)P_\lambda(\cos\theta_k). \tag{1}$$

The v_λ were obtained by inverting the matrix $P_{k\lambda}=P_\lambda(\cos\theta_k)$. Cubic spline interpolation on the $v_\lambda(R_i)$ coefficients was then used to obtain the potential at any desired point. Given the number of *ab initio* points and their repartition, the resulting potential is very well determined in the region of space accessed by the van der Waals bound states of interest. The minimum of the potential is -69 cm^{-1}, at

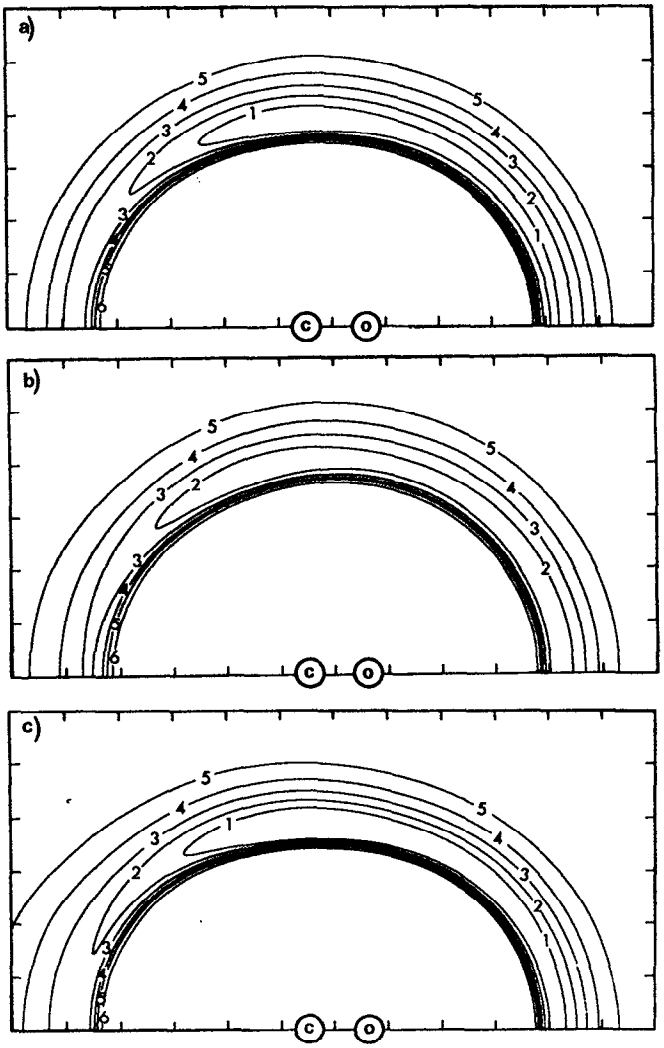

FIG. 2. Equipotentials for Ar···CO. 1, -60 cm^{-1}; 2, -50 cm^{-1}; 3, -40 cm^{-1}; 4, -30 cm^{-1}; 5, -20 cm^{-1}; 6, 0 cm^{-1}. Energies are with respect to Ar+CO($v=0$). The origin is at the center of mass of CO, and the C and O atoms are represented along the abscissas axis. The contours correspond to the value of the potential at the position of the Ar atom in the ArCO plane (a) *ab initio*; (b) lower anisotropy variation [see text, Eq. (11)]; (c) higher anisotropy variation [see text, Eq. (12)]. The separation between two consecutive ticks on the grid is 1 Å. The coordinates of the minima are the following: (a) $R_e=4.0$ Å, $\theta_e=100°$, $V(R_e,\theta_e)=-68.51$ cm^{-1}; (b) $R_e=4.1$ Å, $\theta_e=110°$, $V(R_e,\theta_e)=-58.14$ cm^{-1}; (c) $R_e=3.9$ Å, $\theta_e=100°$, $V(R_e,\theta_e)=-77.73$ cm^{-1}.

$R_e=4.0$ Å and $\theta_e=100°$. However, the potential around this minimum is very flat since at ($R=3.8$ Å, $\theta=90°$), $V_{\mathrm{Ar}\cdots\mathrm{CO}}=-68$ cm^{-1}, and at ($R=4.0$ Å, $\theta=110°$), $V_{\mathrm{Ar}\cdots\mathrm{CO}}=-68$ cm^{-1}. [In this paper the energy reference is the asymptotic limit Ar+CO ($v_{\mathrm{CO}}=0$) unless otherwise specified.]

III. METHODOLOGY FOR THE CALCULATED SPECTRUM

Since the *ab initio* potential for the Ar–CO interaction was calculated with CO frozen at its equilibrium distance,[20] it could not provide any information on the r (CO vibrational

Downloaded 19 Aug 2003 to 128.125.187.57. Redistribution subject to AIP license or copyright, see http://ojps.aip.org/jcpo/jcpcr.jsp

coordinate) dependence. In addition, Shin *et al.* have shown that less than 2% of the binding energy at the potential minimum was due to electrical properties. Hence it was not realistic to model a vibrational dependence of the (weak) dipole moment of CO to get an r-dependence of the interaction potential. We thus performed the calculation of the infrared spectrum of the Ar···CO complex with CO frozen at its equilibrium distance. This is considered to be a good approximation since the van der Waals and rotational degrees of freedom have a frequency at least two orders of magnitude lower than the CO vibration. The consequences of this approximation are that we cannot calculate the shift of the Ar···CO with respect to the CO spectrum, nor can we get the variation of the average structural parameters with the vibrational level of CO. From the experimental results of McKellar *et al.* (Table VII in Ref. 22), the relative variation of the effective B_v rotational constant of the complex between $v_{CO}=0$ and $v_{CO}=1$ is less than 0.3%. Also, the estimated shift of the complex absorption is -0.440 cm^{-1} from the unperturbed CO origin, which is very small compared to the CO vibrational frequency (2143 cm^{-1}). This is also observed in the shift of the CO vibrational excitation frequency in an argon matrix.[26] Hence the Ar···CO intermolecular potential depends very little on the CO vibrational excitation. The method we used for calculating the Ar···CO spectrum is derived from the one used in calculating the rovibrational absorption spectra of rare gas–Cl_2 complexes[27] and is now standard. It is very similar to the one used by Clary and Nesbitt in their calculation of vibration-rotation spectra for rare gas–HCl complexes.[15] The rovibrational bound states are calculated using conventional basis set methods and the transition dipole moment is carried by the diatomic and assumed to be unaffected by the presence of the rare gas atom. We recall here the main points of the method, in order to make clear which assumptions are made, to specify notations, and to give computational details.

A. ArCO bound states

We have used the Hamiltonian in Jacobi coordinates

$$H=-\frac{\hbar^2}{2m}\frac{\partial^2}{\partial R^2}+\frac{B_{CO}}{\hbar^2}j^2+\frac{l^2}{2mR^2}+V_{Ar\cdots CO}(R,\theta), \quad (2)$$

where $m=M_{Ar}M_{CO}/(M_{Ar}+M_{CO})$ is the reduced mass of the complex, $\mathbf{R}$ is the vector going from the center of mass of CO to the Ar atom, B_{CO} is the rotational constant of CO taken as B_e from Ref. 28 ($B_{CO}=1.9313$ cm^{-1}), $\mathbf{j}$ is the rotational angular momentum of CO and l is the angular momentum associated with $\mathbf{R}$. Finally, $V_{Ar\cdots CO}(R,\theta)$ is the CO···Ar interaction potential (going to zero as R goes to infinity), and θ is the angle between the CO axis and $\mathbf{R}$ (see Fig. 1). Apart from freezing the CO vibration, it is the exact Hamiltonian for this system (as is usual in this type of study, the total wave function has been divided by R).

In order to calculate the rotational spectrum we introduce the total angular momentum

$$\mathbf{J}=\mathbf{j}+\mathbf{l}. \quad (3)$$

Using the body-fixed system in which the z axis is attached to $\mathbf{R}$, the angular basis functions are

$$\langle\hat{R},\hat{r}|JM\Omega j\rangle=\sqrt{\frac{2J+1}{4\pi}}D^{J*}_{M\Omega}(\varphi_R,\theta_R,0)Y_{j\Omega}(\theta,\varphi) \quad (4)$$

which are eigenfunctions of J^2, J_z, j^2, and $J_z(=j_z)$, with eigenvalues $\hbar^2J(J+1)$, $\hbar M$, $\hbar^2j(j+1)$, and $\hbar\Omega$, respectively. In Eq. (4), φ_R and θ_R are the spherical angular coordinates of $\mathbf{R}$ in the space-fixed axes (X,Y,Z), while φ and θ are the spherical angular coordinates of $\mathbf{r}$ in the body-fixed axes (x,y,z). $D^J_{M\Omega}$ denotes a Wigner function and $Y_{j\Omega}$ a spherical harmonic. The parity-adapted basis functions are

$$|JM\Omega jp\rangle=\begin{cases}\dfrac{1}{\sqrt{2}}\{|JM\Omega j\rangle+p(-1)^J|JM,-\Omega,j\rangle\} \\ \quad \text{for} \quad \Omega>0; \\ |JM\Omega=0,j\rangle \quad \text{for} \quad \Omega=0.\end{cases} \quad (5)$$

which have parity p under inversion of all coordinates through the origin. In the Hamiltonian of Eq. (2), l^2 is then replaced by

$$l^2=(\mathbf{J}-\mathbf{j})^2=J^2+j^2-2j_zJ_z-j_+J_--j_-J_+, \quad (6)$$

where $j_\pm$ stands for $j_x\pm ij_y$ and $J_\pm$ for $J_x\pm iJ_y$.

The stretching basis functions $\phi_n(R)$ were chosen as harmonic oscillator functions centered at $R_e=4.0$ Å, with a frequency $\hbar\omega=24.5$ cm^{-1} (this parameter was obtained by fitting the energy difference of the first two levels of a one-dimensional calculation performed at $\theta=\theta_e=100°$ with the harmonic formula). The energy of a given level (v,JMp) (where v is a collective index labeling the van der Waals levels) and the coefficients of the expansion of its wave function onto the product basis set

$$\Phi^{JMp}_v=\sum_\Omega\sum_j\sum_n C^{Jp}_{v,\Omega jn}\phi_n|JM\Omega jp\rangle \quad (7)$$

are determined by diagonalizing the Hamiltonian matrix [C does not depend on M since the Hamiltonian in Eq. (2) is invariant under rotation of the complex in space]. Ten harmonic oscillator functions and ten angular basis functions were used, and the energies of the levels implied in the spectrum were converged to better than 0.01 cm^{-1}.

B. Coriolis decoupling

In order to simplify the spectrum calculation, Coriolis decoupling approximation was tested on the bound states. In this approximation the off-diagonal terms of l^2, i.e., j_+J_- and j_-J_+, are neglected in Eq. (6). The projection quantum number of $\mathbf{J}$ onto the body-fixed axis z, Ω, is then a good quantum number, and the sum in Eq. (7) no longer runs over Ω,

$$\Phi^{JM\Omega}_v=\sum_j\sum_n C^{J\Omega}_{v,jn}\phi_n|JM\Omega j\rangle. \quad (8)$$

Comparison with the result of the exact calculation showed that this is a good approximation for the level of accuracy wanted here, since uncertainty on the potential is expected to be larger than errors on the energies due to Coriolis coupling. For example, for $J=9$, the ground level is at -45.24 cm^{-1} (i.e., 5.59 cm^{-1} above the $J=0$ ground level), and it is

Downloaded 19 Aug 2003 to 128.125.187.57. Redistribution subject to AIP license or copyright, see http://ojps.aip.org/jcpo/jcpcr.jsp

99.2% $\Omega=0$. The Coriolis decoupled result is $-45.20\ \mathrm{cm}^{-1}$ for the energy of the $J=9$, $\Omega=0$ level, which corresponds to an error of $0.04\ \mathrm{cm}^{-1}$. Note however that the experimental uncertainty on line positions is two orders of magnitude smaller.[22] The result of Coriolis coupling could also be to perturb transition intensities. However, as shown by the example of the ground $J=9$ level above, the wave functions are almost pure in Ω hence these perturbations were neglected.

C. Spectrum calculation

Using these bound states both for $v_{CO}=1$ and $v_{CO}=0$ (since the CO vibration is frozen), we have calculated the infrared spectrum with the Coriolis decoupling approximation. The transition dipole moment was assumed to be carried by the CO molecule, the van der Waals vibrations inducing a much smaller variation of the dipole moment. The transition dipole moment operator is then written as[30]

$$\boldsymbol{\varepsilon}\cdot\boldsymbol{\mu}=\varepsilon\mu_{CO}\sum_{q} D^{1*}_{0q}(\varphi_R,\theta_R,0)D^{1*}_{q0}(\varphi,\theta,0). \tag{9}$$

The matrix elements of this transition operator between the Coriolis decoupled basis functions are given in Appendix A, together with the intensity calculation.

D. Rigid rotor and free internal rotor limits

In a very interesting paper, Nesbitt and Naaman[29] have shown that if only a small fraction of the bound states of a complex are determined (as in a supersonic jet experiment), then they can often be well fit to a rigid rotor Hamiltonian, even in extremely floppy molecular systems with wide amplitude vibrational motions. The case of Ar···CO is expected to be close to their model of a pinwheel (nearly-free internal rotor). Hence in order to ascertain whether the Ar···CO spectrum could be considered as closer to a rigid rotor spectrum or to a free internal rotor, we have made the following checks: we have fitted the rovibrational energy levels from the bound state calculation to rotational constants (which also served to compare the calculated results to the experimental ones, see Sec. IV, since the experimental results do not give intensities); and we have compared the calculated spectrum to the two limiting approximations, the free CO internal rotor and the rigid Ar···CO spectrum.

The free internal rotor limit, in which the CO molecule freely rotates inside the complex, is obtained in the limit of very low anisotropy of the Ar···CO interaction, where j becomes a good quantum number. The resulting spectrum is identical to the free rotor spectrum of the uncomplexed CO molecule, since the transition dipole moment is carried by CO.

In order to compare the calculated spectrum with the limit in which the Ar···CO complex could be considered as rigid, we had to select a structure for the rigid approximation to Ar···CO. This could not be extracted from the fitted rotational constants since A could not be determined (see Sec. IV). We have chosen two reasonable configurations. The first one is the minimum energy configuration, $R_e=4.0$ Å, $\theta_e=100°$. The second one is obtained by vibrationally averaging the quantities $\cos^2\theta$ and R^2 over the $J=0$ zero-point level wave function Φ_0^{000}. Explicitely, the values $R_0=4.06$ Å and $\theta_0=52.2°$ for this configuration were determined from

$$\cos^2\theta_0=\langle\Phi_0^{000}|\cos^2\theta|\Phi_0^{000}\rangle,$$
$$R_0^2=\langle\Phi_0^{000}|R^2|\Phi_0^{000}\rangle. \tag{10}$$

This choice is not crucial for R since averaging R, R^2, or R^{-2} gives approximately the same value (see Table I). It is however determinant for θ as is obvious from the same table, which shows that the floppiness in Ar···CO mainly resides in the angular motion. We chose this rather than inverting the expectation values for the inverse of the moments of inertia, because we could then compare directly to the microwave results of Ogata *et al.*[23] which give a measure of $\cos^2\theta$. Also, $\cos^2\theta$ and R^2 are the quantities appearing in the inertia tensor (given in Appendix B together with the rotational constants). For the relationship between θ and experimentally deduced structural properties, see Ref. 31.

TABLE I. Averaged values of the first powers of $\cos\theta$ and R in the $J=0$ ground level Φ_0^{000}. $\bar{\theta}_n$ stands for arccos $({}^n\sqrt{\langle\cos^n\theta\rangle})$. The equilibrium structure is given in the first line for comparison.

n	$\langle R^n\rangle$(Å^n)	${}^n\sqrt{\langle R^n\rangle}$(Å)	$\langle\cos^n\theta\rangle$	$\bar{\theta}_n$
e	···	4.0	···	100°
1	4.058	4.058	0.1497	81.4°
2	16.4952	4.061	0.3762	52.3°
−2	0.0610	4.046	···	···

E. Sensitivity to the potential anisotropy

In order to check how sensitive the results are to the anisotropy of the *ab initio* potential, we have reproduced the calculated spectrum with a lower and a higher anisotropy. The spectrum for the less anisotropic (l.a.) potential was obtained by multiplying the coefficients $v_\lambda(R)$, $\lambda>0$ in the expansion (1) of the potential by 0.5

$$v_\lambda^{\text{l.a.}}(R)=0.5v_\lambda(R),\quad \lambda>0. \tag{11}$$

For the more anisotropic (h.a.) potential, just multiplying the $v_\lambda(R)$, $\lambda>0$ coefficients by 1.5 at all distances gave spurious oscillations in the repulsive part of the potential. We used a switching function to smooth it at short distances

$$v_\lambda^{\text{h.a.}}(R)=v_\lambda(R)\left\{1+\frac{\alpha}{2}\left[1+\tanh\left(\frac{R-R_0}{\Delta R}\right)\right]\right\},\quad \lambda>0. \tag{12}$$

TABLE II. Rotational constants (in cm^{-1}) of Ar···CO for the rigid spectra, and angle α between the molecular axes and the inertia axes (see Appendix B). The first line corresponds to the configuration at the minimum of the potential energy surface, and the second to the averaged configuration of the ground $J=0$ van der Waals level. The experimental value for $|\alpha|$ is 1.2° (Ref. 23).

	A	B	C	α(°)
$R_e=4.0$ Å, $\theta_e=100.°$	1.9894	0.0639	0.0619	0.334
$R_0=4.061$ Å, $\theta_0=52.3°$	3.0588	0.0613	0.0601	−0.898

Downloaded 19 Aug 2003 to 128.125.187.57. Redistribution subject to AIP license or copyright, see http://ojps.aip.org/jcpo/jcpcr.jsp

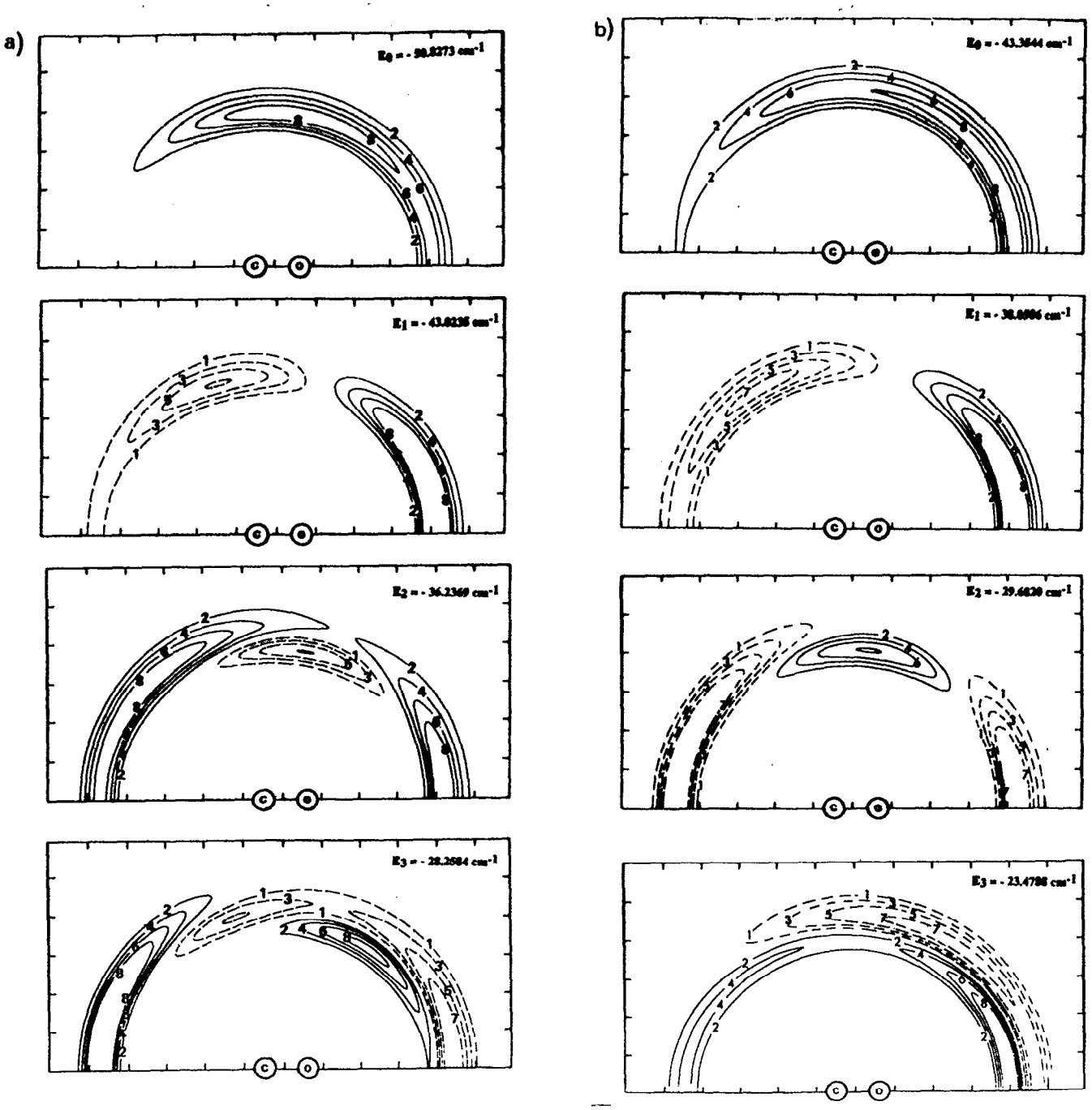

FIG. 3. Contours of the wave functions for the first four levels ($J=0$) of Ar···CO. The origin is at the center of mass of CO, and the C and O atoms are represented along the abscissas axis. The separation between two consecutive ticks on the grid is 1 Å. The contours correspond to the value of the wave function at a given position of the Ar atom in the ArCO plane, with dotted contours representing negative values. The wave functions are calculated for (a) the *ab initio* potential; (b) the lower anisotropy variation [see text, Eq. (11)]; (c) higher anisotropy variation [see text, Eq. (12)], respectively. Energies are indicated as E_v in each plot. Contour key: 1, −0.10; 2, 0.10; 3, −0.20; 4, 0.20; 5, −0.03; 6, 0.30; 7, −0.40; 8, 0.40.

The values for the parameters of the switching function are the following: $R_0=4.0$ Å, $\Delta R=0.5$ Å, and $\alpha=0.5$. The equipotentials for the lower and higher anisotropy case are presented in Figs. 2(b) and 2(c), respectively.

IV. RESULTS AND DISCUSSION

A. Bound state wave functions

The wave functions of the first four $J=0$ levels are presented in Fig. 3(a). As expected from the shape of the *ab initio* potential, the ground state wave function is extremely delocalized, allowing for contourning the CO axis on the oxygen end but not on the carbon end. Its energy is $E_0=-50.827$ cm^{-1}, which corresponds to a zero-point energy of 17.68 cm^{-1}. The extreme floppiness of the complex even in the ground level is revealed by the values obtained for the average of powers of R and θ, calculated as in Eq. (10); the results are given in Table I. The first excited level, at -43.024 cm^{-1} (i.e., 7.803 cm^{-1} above the ground level)

Downloaded 19 Aug 2003 to 128.125.187.57. Redistribution subject to AIP license or copyright, see http://ojps.aip.org/jcpo/jcpcr.jsp

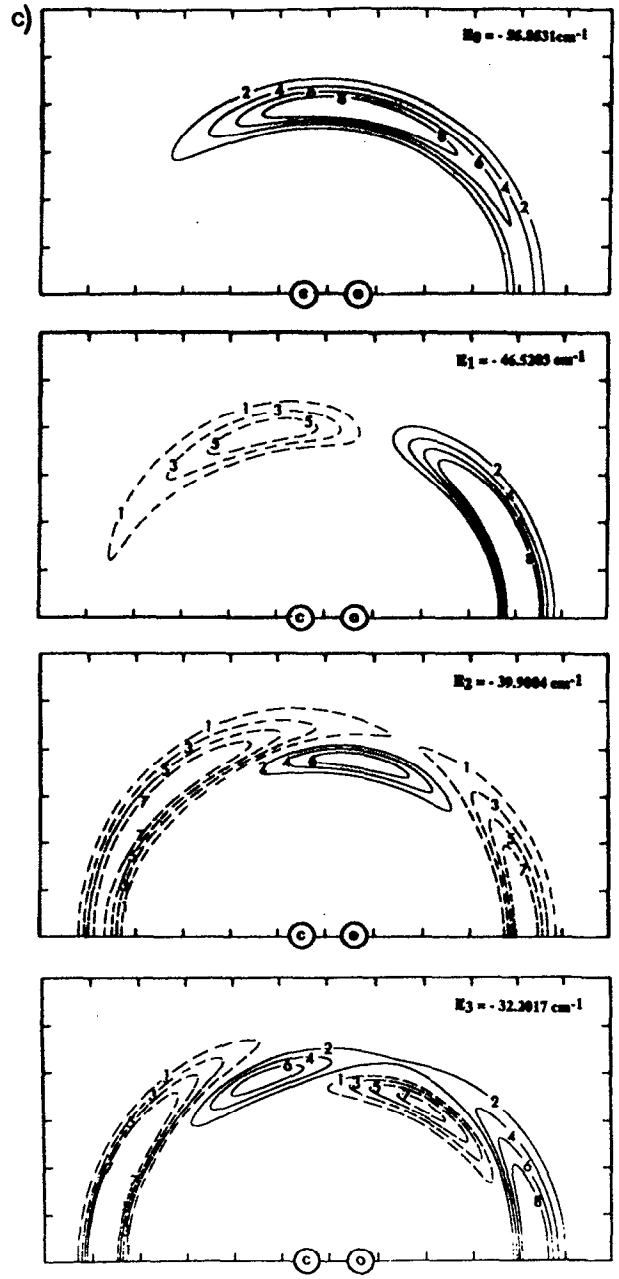

FIG. 3. (*Continued.*)

corresponds to a bending excitation, as can be seen from the node in the angular coordinate. The second excited level, at -36.237 cm^{-1} (14.590 cm^{-1} above the ground level) is already a combination of bending and stretching excitation, as can be seen from the shape of its wave function, but is still mainly two quanta of bending excitation. Note that assuming harmonic behavior, the first stretching excitation would be expected at -23.27 cm^{-1} (27.56 cm^{-1} above the ground level). The one-dimensional determination of the stretching frequency at θ_e has given 24.5 cm^{-1}. The next levels, at -28.26 and -25.33 cm^{-1} (22.57 and 25.50 cm^{-1} above the zero-point level), can be assigned to three quanta and four quanta of bending excitation, respectively, mixed with one quantum of stretching. Higher levels are even more mixed and not assignable in terms of stretching and bending motions.

In their analysis of the experimental infrared spectrum of Ar···CO, McKellar *et al.*[22] have used a quasirigid rotor formula for the energy levels of this complex

$$E_{\mathrm{rot}}(J,K)=E_0(K)+\bar{B}[J(J+1)-K^2]-D[J(J+1)-K^2]^2 +H[J(J+1)-K^2]^3+\Delta E_K, \tag{13}$$

where $\bar{B}=(B+C)/2$, K stands for K_a, and ΔE_K is the asymmetry splitting term. In order to compare with their results, we have fitted the energy of the ground state of each of our Ω stack of J levels to the same formula. Since we are using Coriolis decoupling, Ω is considered as a good quantum number and it should coincide with K_a in the limit of a symmetric rigid rotor. Hence ΔE_K is zero and the fit was made only on $E_0(K)$, $\bar{B}$, D, and H. The resulting constants are presented in Table III, compared with the experimental results of McKellar *et al.*[22] We have included all the $J\leqslant 15$ levels in the fit, since $J=15$ was the highest J level with a non-negligible population at the temperature ($T=5$ K) of the calculated spectrum. A sensitivity analysis of the results to the anisotropy of the potential is also included. It corresponds to the constants obtained by fitting the energy levels of the potential modified according to Eqs. (11) and (12) in order to make it less or more anisotropic.

The first conclusion that we can draw from this table is that the rotational "constants" do vary with Ω, as they do with K in the experiment, although they are well defined for a given Ω subband. They decrease with Ω, which is also the experimental result. The strongest variation is for A [value deduced from $E_0(\Omega)=A\Omega^2$], which is very sensitive to the value of the angle θ (see the constants of inertia in Appendix B), hence to the angular distribution of the bound state wave function. The relative variation is more important in the less anisotropic potential, as expected, and the average value larger. The experimental result seems to correspond to a more anisotropic potential than even the more anisotropic one studied here (both for the relative variation and absolute value of A). This is also true for the absolute value of B. The centrifugal distortion constants D and H of the *ab initio* potential and its more anisotropic variation have the right order of magnitude, except for the higher Ω levels.

The comparison with the bound states obtained by Tennyson *et al.*[25] from Mirsky's potential[18] shows that Shin's *ab initio* potential[20] gives a much weaker van der Waals bond. Tennyson *et al.* find the $J=0$ ground level at -84.6 cm^{-1}, with the first bending and stretching excitations at 14.3 and 24.2 cm^{-1}, respectively. Despite this tighter bonding, they reach a conclusion similar to ours; that the identities of the vibrational states rapidly become confused as the bend and the stretch are excited. As put by McKellar *et al.*,[22] this "serves as a reminder that Ar···CO cannot be treated simply as a normal semirigid molecule, especially in its excited states." This is very different from the complexes of the

Downloaded 19 Aug 2003 to 128.125.187.57. Redistribution subject to AIP license or copyright, see http://ojps.aip.org/jcpo/jcpcr.jsp

TABLE III. Rotational constants (cm^{-1}) obtained by fitting the energy levels to Eq. (13) for the *ab initio* potential (Ref. 20); sensitivity to the potential anisotropy [see text, and Eqs. (11) and (12)] and comparison with the ones obtained by McKellar *et al.* (Ref. 22).

		This calculation			Experimental
K		*Ab initio*	Higher anisotropy[a]	Lower anisotropy[b]	McKellar *et al.*
0	$\bar{B}$	0.062 7478	0.064 8506	0.057 3928	0.069 089(6)
	D	0.2599×10^{-5}	0.2287×10^{-5}	0.2086×10^{-5}	$0.1913(20)\times10^{-5}$
	H	-0.492×10^{-9}	-0.515×10^{-9}	-0.347×10^{-9}	$-0.463(18)\times10^{-9}$
	A[c]	···	···	···	···
1	$\bar{B}$	0.063 1849	0.065 2078	0.057 5336	0.068 776(6)
	D	0.2528×10^{-5}	0.2168×10^{-5}	0.2063×10^{-5}	$0.2030(21)\times10^{-5}$
	H	-0.500×10^{-9}	-0.477×10^{-9}	-0.254×10^{-9}	$-0.506(21)\times10^{-9}$
	A[c]	2.943	2.696	3.534	2.40
2	$\bar{B}$	0.063 4376	0.065 4146	0.057 7503	0.067 909(7)
	D	0.2436×10^{-5}	0.2096×10^{-5}	0.1978×10^{-5}	$0.2369(26)\times10^{-5}$
	H	-0.393×10^{-9}	-0.378×10^{-9}	-0.231×10^{-9}	$-1.545(32)\times10^{-9}$
	A[c]	2.504	2.402	2.758	2.23
3	$\bar{B}$	0.063 6649	0.065 5924	0.057 9337	0.066 643(4)
	D	0.2335×10^{-5}	0.2014×10^{-5}	0.1936×10^{-5}	0.3111×10^{-5}
	H	-0.330×10^{-9}	-0.304×10^{-9}	-0.232×10^{-9}	-6.61×10^{-9}
	A[c]	2.348	2.288	2.502	2.16

[a]See text, Eq. (12).
[b]See text, Eq. (11).
[c]Deduced from $E_0(K)=AK^2$.

dihalogen molecules with rare gas atoms for example, where the bound states can be fitted within a good approximation by a rigid rotor formula.[10–13]

The microwave spectra of Ogata *et al.*[23] give very good indications on the structure of the ground state. Like for the infrared spectrum, the average equilibrium intermolecular distance is found to be shorter than the one we get from the *ab initio* potential (3.811 Å instead of 4.06 Å). Concerning the average value of the angle θ, a problem of definition similar to ours is encountered, due to the large amplitude motion involved. Three different models were used. All three gave results compatible with the argon atom being on average closer to the oxygen, but with three rather different values for θ. The first model was fitting R and θ to reproduce the experimental values of $\bar{B}$ for the CO isotopic variations of Ar···CO and gave $R=3.811$ Å and $\theta=80.2\pm6.3°$. In the second model, R was held fixed at the value obtained from the first model, and θ was obtained by reproducing A (from the infrared experiment of McKellar *et al.*[22]) and $\bar{B}$, which gave $\theta=62.3°$. Yet a third measure of θ was obtained from the ^{17}O quadrupole coupling constant and gave $\theta=69.5°$. As can be seen from Table I, all these results fall within the two extreme values we obtain from calculating the average value of $\cos\theta$ (81.4°) or $\cos^2\theta$ (52.3°). The value for the angle α

TABLE IV. Energy (cm^{-1}) of the first five levels of Ar···CO as a function of Ω and J for the *ab initio* potential of Shin (Ref. 20), and a lower and higher anisotropy variation [see text, Eqs. (11) and (12)].

		$\Omega=0$				$\Omega=1$			$\Omega=2$		$\Omega=3$
	v	$J=0$	1	2	3	$J=1$	2	3	$J=2$	3	$J=3$
	0	−50.827	−50.702	−50.451	−50.075	−47.821	−47.568	−47.189	−40.685	−40.304	−29.503
Ab initio	1	−43.024	−42.905	−42.669	−42.316	−36.339	−36.102	−35.748	−26.161	−25.805	−12.491
	2	−36.237	−36.126	−35.904	−35.570	−30.184	−29.953	−29.606	−20.581	−20.230	−7.307
	3	−28.258	−28.150	−27.933	−27.609	−21.235	−21.015	−20.685	−10.011	−9.676	···
	4	−25.329	−25.214	−24.986	−24.644	−16.882	−16.658	−16.324	−5.972	−5.643	···
	0	−43.354	−43.240	−43.010	−42.666	−39.763	−39.533	−39.188	−32.208	−31.862	−20.660
Lower	1	−38.059	−37.947	−37.724	−37.390	−30.927	−30.702	−30.365	−19.663	−19.323	−4.528
anisotropy	2	−29.682	−29.574	−29.360	−29.037	−22.163	−21.949	−21.627	−13.569	−13.251	−1.606
	3	−23.479	−23.374	−23.165	−22.851	−17.089	−16.874	−16.552	−3.728	−3.402	···
	4	−20.989	−20.881	−20.666	−20.343	−12.106	−11.895	−11.578	−0.018	···	···
	0	−55.853	−55.723	−55.464	−55.075	−53.091	−52.831	−52.440	−46.113	−45.720	−35.062
Higher	1	−46.520	−46.400	−46.158	−45.797	−40.013	−39.771	−39.408	−30.174	−29.811	−16.708
anisotropy	2	−39.900	−39.789	−39.567	−39.234	−33.925	−33.690	−33.339	−23.914	−23.553	−10.329
	3	−32.202	−32.093	−31.875	−31.548	−24.562	−24.340	−24.008	−13.599	−13.262	···
	4	−27.305	−27.186	−26.950	−26.595	−18.778	−18.549	−18.206	−7.781	−7.448	···

Downloaded 19 Aug 2003 to 128.125.187.57. Redistribution subject to AIP license or copyright, see http://ojps.aip.org/jcpo/jcpcr.jsp

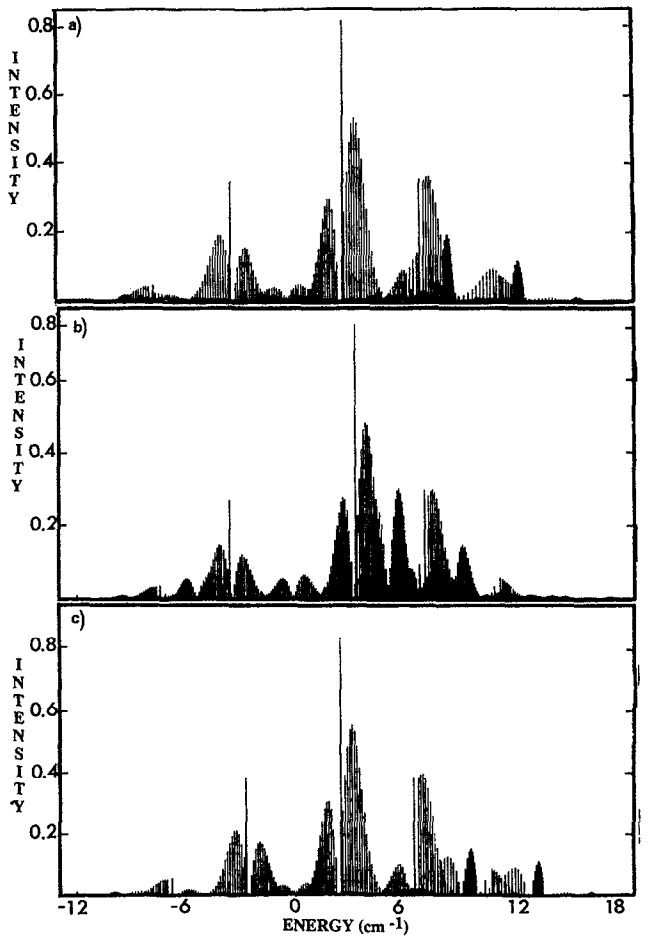

FIG. 4. Rotational spectrum calculated at 5 K for (a) the *ab initio* potential; (b) the lower anisotropy variation [see text, Eq. (11)]; (c) the higher anisotropy variation [see text, Eq. (12)], respectively. The zero is at the center of the CO $v_{CO}=1\leftarrow 0$ transition. Since there is no spectral shift of the complex with respect to CO in this calculation, it is also at the center of the Ar···CO($v_{CO}=1\leftarrow 0$) transition. Intensities are in arbitrary units, but the same unit is kept for all plots.

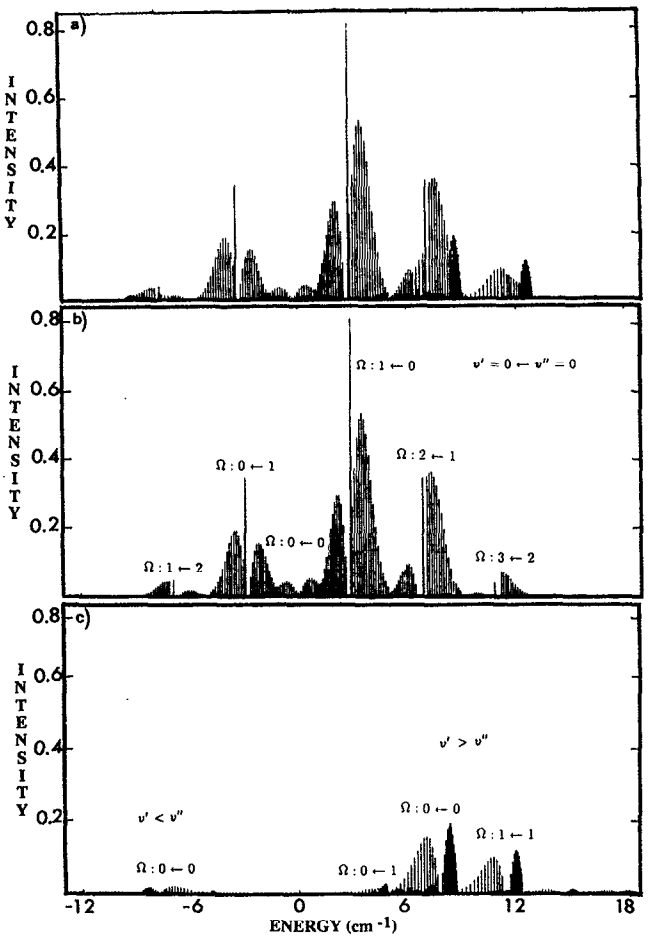

FIG. 5. Infrared absorption spectrum calculated at 5 K. (a) Reproduction of the global spectrum of Fig. 4(a); (b) only the transitions from $v''=0$ to $v'=0$; (c) only the transitions from v'' to $v'>v''$ (progressions on the van der Waals bending mode) and from v'' to $v'<v''$ (hot bands). Intensities are in arbitrary units, but the same scale is kept for all plots.

between the a inertia axis and the axis parallel to **R** [see calculation in Appendix B, Eq. (B3)] is $\alpha_e=0.334°$ for the equilibrium geometry, and $\alpha_0=-0.898°$ for the averaged geometry. In their microwave study, Ogata *et al.*[23] have obtained $|\alpha|=1.2°$, which is closer to the result for the averaged geometry.

Ogata *et al.* also note a strong similarity in both the θ and R values obtained for the van der Waals complex of N_2, isoelectronic to CO, and Ar in the microwave study of Jäger and Gerry;[32] they found a perpendicular geometry for the complex, confirming the results of infrared measurements by Henderson and Ewing,[33] and by McKellar.[34] They calculated a distance of 3.865 Å between the argon atom and the center of mass of the nitrogen molecule, and estimated the average angular displacement of the N_2 subunit from the linear configuration, defined by $\theta=\arccos[\langle\cos^2\theta\rangle]^{1/2}$, to be 68.3°.

Havenith *et al.*[24] have measured the infrared spectrum of Ar···CO and they could detect the transition from the ground van der Waals level, $v_{CO}=0$, $K=0$, to the first excited bending state, $v_{CO}=1$, $K=0$. They found that there is no Q branch for this transition, and that the first excited $K=0$ bending state of Ar···CO lies at 11.914 cm^{-1} above the $K=0$ ground state. Because of the extreme floppiness of this complex, the energies of the levels corresponding to excitation in the angular coordinate are very dependent on Ω. This can be seen from Table IV, which presents the first five levels for each (J,Ω), $J\leqslant 3$, $\Omega\leqslant 3$ value for the *ab initio* potential and its lower and higher anisotropy variation. For $J=0$ the first excited bending state is at 7.804 cm^{-1} above the ground $J=0$ state. This is not in very good agreement with the experimental result. Even the higher anisotropy version of the potential gives only 9.333 cm^{-1} for the $\Omega=0$ bending excitation. For $\Omega=1$, $J=1$, the first excited level is at 11.482 cm^{-1} above the ground $\Omega=1$, $J=1$ van der Waals level. This shows that there is no bending frequency to speak of in such a flat angular potential.

Downloaded 19 Aug 2003 to 128.125.187.57. Redistribution subject to AIP license or copyright, see http://ojps.aip.org/jcpo/jcpcr.jsp

B. ArCO rotational spectrum

The rotational spectrum calculated at 5 K is shown in Fig. 4(a). It has the overall appearance of the spectrum for a nearly prolate symmetric top molecule (for which K_a is a good quantum number); it consists mainly of $\Delta\Omega=\pm1$ (perpendicular) branches, with a very weak $\Delta\Omega=0$ (parallel) branch. Since the dipole is carried by the CO molecule, it means that on average, CO is mainly perpendicular to the intermolecular axis. Each Ω (P or R) branch is then divided into three J subbranches, P, Q, and R. If one tries to assign rotational constants to this spectrum, however, one can use an effective $\bar{B}$ [$=(B+C)/2$] constant but it changes with Ω, and there is no equivalent for the A constant, the spacings between the Ω branches changing with Ω'' (see the discussion on the comparison of the energy levels with rigid or semirigid rotor levels).

In addition, there are some other bands. These are clearly seen in Fig. 5, which presents a decomposition of the spectrum in Fig. 4(a). The spectrum of Fig. 4(a) is reproduced in Fig. 5(a), while only the transitions that originate from the ground van der Waals level of the (J'',Ω'') and go to the ground level of the (J',Ω') manifolds are shown in Fig. 5(b), and Fig. 5(c) shows only the transitions from v'' to $v'>v''$ (progression on the van der Waals modes), or from v'' to $v'<v''$ (hot bands). There are hot bands, but with a very low intensity at the temperature of this spectrum (at 5 K, the Boltzmann factor for the population of the first excited level, which is the 7.8 cm^{-1} bending vibration, would be 0.1). Of course they will be more important at higher temperatures (the same factor becomes 0.3 at 10 K, which was the approximate temperature in the supersonic jet/laser spectra,[22] and 0.8 at 60 K which was the approximate temperature in the long path Fourier transform spectra[22]). The additional bands that clearly appear in the spectrum correspond to excitation of a van der Waals mode. The origin for the first one is 7.80 cm^{-1}, it is the $(\Omega'=0\leftarrow\Omega''=0)$ branch for bending excitation. It has a bandhead in the R branch, at 8.739 cm^{-1} for $J=14$, and no Q branch. This is in agreement with the observation by Havenith *et al.*,[24] who could detect this transition and show that it did not have a Q branch, but at a higher frequency. Excitation of the mode at 14.6 cm^{-1} is not seen. The other bands correspond to the other Ω branches for the same bending excitation. In particular, the $(\Omega'=1\leftarrow\Omega''=1)$ branch is at 11.482 cm^{-1}. It is particularly interesting to note that in this case, the parallel bands are the ones getting most of the intensity. Transitions involving excited bending or stretching states of the complex were invoked by McKellar *et al.*[22] to explain why only a small fraction of the total number of lines had been accounted for in the Fourier transform spectra.

C. Comparison with the free rotor spectrum

The spectrum in the limit of CO freely rotating (i.e., the limit where the Ar···CO interaction potential is isotropic) would be identical to the uncomplexed CO spectrum, since the dipole moment is carried by CO. In addition, there can be no progressions on the van der Waals stretching mode since the potential was taken to be the same for $v=0$ and $v=1$.

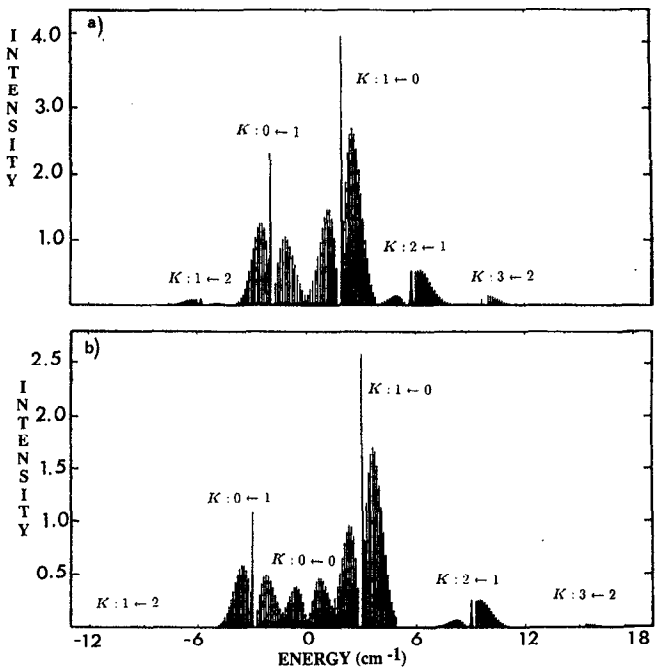

FIG. 6. Rigid rotor spectrum at 5 K. Ar···CO is frozen at (a) the configuration of the minimum of the potential, $R_e=4.0$ Å, $\theta_e=100°$ (the corresponding rotational constants are $A=1.9894$ cm^{-1}, $B=0.0639$ cm^{-1}, $C=0.0619$ cm^{-1}); (b) the averaged configuration of the $J=0$ zero-point level, $R_0=4.061$ Å, $\theta_0=52.3°$ (the corresponding rotational constants are $A=3.0588$ cm^{-1}, $B=0.0613$ cm^{-1}, $C=0.0601$ cm^{-1}). Intensity is in arbitrary units, but with the same scale as in (a).

Hence the spectrum would just be the one of a diatomic, with a P and an R branch ($\Delta j=\pm1$) and a spacing equal to $2B_{CO}$ between two adjacent lines, where $B_{CO}=1.9313$ cm^{-1} (from Ref. 28). This is clearly not the case and the spectrum exhibits a lot more lines, although the ground $J=0$ state contains $\simeq80\%$ $j=0$. The first excited bending state, which should correlate with $j=1$, is at 7.8 cm^{-1} above the ground state, i.e., about twice the energy of the corresponding free rotor level.

D. Comparison with the rigid rotor spectrum

The rigid rotor spectrum for Ar···CO frozen at the configuration of the minimum of the potential is shown in Fig. 6(a). The corresponding moments of inertia are given in Table II. It is a nearly symmetric prolate top ($A\gg B\simeq C$) with the axis of smallest inertia parallel to z, the intermolecular axis. Hence the transition dipole moment is almost perpendicular to the symmetry axis ($\theta_e=100°$), and almost no $\Delta K=0$ transition is observed. The difference with the non rigid spectrum is mainly that the A constant is smaller than the spacings between the origin of the non rigid spectrum and the $\Omega=1\leftarrow0$ band origin. Also, as expressed above, the nonrigid spectrum cannot be assigned an A constant to give the $\Delta\Omega=\pm1$ band origins. This is different from the result found by Nesbitt and Naaman[29] in their nearly-free internal rotor ("pinwheel") model, where they found that even for an extremely floppy molecule the rotational spectrum at low

Downloaded 19 Aug 2003 to 128.125.187.57. Redistribution subject to AIP license or copyright, see http://ojps.aip.org/jcpo/jcpcr.jsp

temperature could be fitted with a rigid rotor Hamiltonian (although giving somewhat aberrant rotational constants). In addition, progressions and hot bands on the van der Waals bending modes could not be seen in a rigid rotor spectrum since the interaction potentials were taken as identical in the $v_{CO}=0$ and $v_{CO}=1$ states.

The rigid rotor spectrum for the ground state averaged structure is shown in Fig. 6(b). The corresponding moments of inertia are given in Table II. It is also a nearly prolate symmetric top, but the transition dipole moment carried by CO now has a non-negligible component on the axis of smallest inertia. The result is a significant $\Delta K=0$ band, more intense than the $\Delta\Omega=0$ band observed in the nonrigid spectrum. Also, like in the other rigid spectrum, the A constant is too large and no van der Waals bending progression can be seen.

E. Sensitivity to the potential anisotropy

In order to check the sensitivity of the spectrum to the anisotropy of the potential, we have run again the spectrum calculation with the *ab initio* potential modified according to Eqs. (11) and (12). The resulting spectra are displayed in Figs. 4(b) and 4(c). As could be expected, the lower anisotropy potential gives a lower bending excitation frequency (5.29 cm^{-1} instead of 7.8 cm^{-1}) with a larger free rotor character (the ground level is 91% $j=0$, the first excited one is 78% $j=1$). The higher anisotropy potential gives the inverse result, with a bending frequency of 9.33 cm^{-1}. Also, the free rotor functions are more mixed, with 79% $j=0$ for the ground level and 62% for the first excited one. In addition, the consequence of changing the potential anisotropy on the rotational constants of Eq. (13) has already been discussed. On average, the $\Delta\Omega=\pm1$ subbands are closer together in the higher anisotropy case. Since at the same time the bending frequency is higher, the bending excitation appears in between the $\Omega=2\leftarrow1$ and the $\Omega=3\leftarrow2$ subbands instead of being superimposed with the $\Omega=2\leftarrow1$ subband. The $\Delta\Omega=0$ subband has a lower intensity in the more anisotropic case, reflecting the stronger localization of the wave function in the region of the perpendicular geometry. The comparison with the experimental results of McKellar *et al.*[22] seems to indicate that the potential should be more anisotropic than the *ab initio* one. As can be seen from Table III, the rotational constants obtained from the fit to Eq. (13) are closer to the more anisotropic case. They could not observe a $\Delta\Omega$ subband. And finally, the unassigned lines that they attributed to excited states of Ar···CO overlapped with the $\Omega=3\leftarrow2$ subband. This would correspond to a bending frequency of the order of 11 cm^{-1} which is closer to the 9.33 cm^{-1} found with the more anisotropic modification of the *ab initio* potential. Alternatively, the unassigned lines could correspond to the $\Omega=1\leftarrow1$ bending excitation, but the corresponding $\Omega=0\leftarrow0$ should have been observed around 7.8 cm^{-1}.

V. CONCLUSION

We have calculated the rotational spectrum of Ar···CO from the *ab initio* potential energy surface of Shin *et al.*[20] The spectrum reproduces the essential features of the experimental one by McKellar *et al.*[22] Ar···CO behaves approximately as a T-shaped near prolate symmetric rotor molecule, but the nonrigidity appears in the fact that A is not constant and $\bar{B}$ depends on Ω. The parallel subband is very weak. We have also shown that the additional lines that could not be assigned in the experimental spectrum are due to excitation of the van der Waals bending mode. The band origin for this is predicted to be at 7.803 cm^{-1} from the band origin of the $\Omega=0\leftarrow0$ ground to ground excitation of the complex by the *ab initio* potential, and at 9.33 cm^{-1} by the more anisotropic modification. Although this is not in good agreement with the 11.9143 cm^{-1} experimental results of Havenith *et al.*[24] the very fact that they could observe this transition and that it did not have a Q branch like we noted, shows that the *ab initio* potential reproduces well the main characteristics of the Ar···CO interaction, and in particular its nonrigid character. This floppiness was further evidenced by comparing with rigid rotor spectra corresponding to two different configurations, the one with minimum potential energy, and the one averaged over the ground state. Comparing with what is expected for a free CO internal rotor, we have also shown that the anisotropy of the potential cannot be neglected. However, the Ar–CO equilibrium distance of the *ab initio* potential is larger than the one deduced from the experiment. Also, the more anisotropic modification to the *ab initio* potential seems to be closer to the experimental results. This could indicate that the potential should be slightly more bound than predicted *ab initio*.

ACKNOWLEDGMENTS

V. C. would like to acknowledge a CONICIT fellowship, from the government of Venezuela. S. K. S. thanks the University of California for a Regents's Junior Faculty Fellowship.

APPENDIX A: MATRIX ELEMENTS OF THE TRANSITION DIPOLE MOMENT ATTACHED TO CO BETWEEN CORIOLIS-DECOUPLED BASIS FUNCTIONS; INFRARED ABSORPTION INTENSITIES

Since the transition dipole moment is carried by CO, the transition dipole moment operator can be written as[30]

$$\boldsymbol{\varepsilon}\cdot\boldsymbol{\mu}=\varepsilon\mu_{CO}\sum_{q} D^{1*}_{0q}(\varphi_R,\theta_R,0)D^{1*}_{q0}(\varphi,\theta,0), \tag{A1}$$

where the space-fixed z axis is chosen along the direction of polarization of the exciting light, θ_R and φ_R are the polar angles for $\mathbf{R}$ in the space-fixed frame (X,Y,Z), and θ and φ are the polar angles of $\mathbf{r}$ (the vector going from C to O) in the body-fixed frame (x,y,z). The body-fixed frame is obtained from the space-fixed one by a rotation with Euler angles $(\varphi_R,\theta_R,0)$, using the same convention as in Ref. 35. The matrix elements of this transition operator between the Coriolis decoupled basis functions of Eq. (4) are then

Downloaded 19 Aug 2003 to 128.125.187.57. Redistribution subject to AIP license or copyright, see http://ojps.aip.org/jcpo/jcpcr.jsp

$$\langle J'M'\Omega'j'|\varepsilon\cdot\mu|J''M''\Omega''j''\rangle=\varepsilon\mu_{CO}\sqrt{(2J''+1)(2J'+1)(2j''+1)(2j'+1)}(-1)^{M'}\begin{pmatrix}J' & 1 & J''\\ M' & 0 & -M''\end{pmatrix}\begin{pmatrix}j' & 1 & j''\\ 0 & 0 & 0\end{pmatrix}$$
$$\times\begin{pmatrix}J' & 1 & J''\\ \Omega' & \Omega''-\Omega' & -\Omega''\end{pmatrix}\begin{pmatrix}j' & 1 & j''\\ -\Omega' & \Omega'-\Omega'' & \Omega''\end{pmatrix}. \tag{A2}$$

Using the expression given in Eq. (8) for the wave function, the intensity for the $(v_{CO}=1,J',M',\Omega',v')\leftarrow(v_{CO}=0,J'',M'',\Omega'',v'')$ transition is proportional to

$$\mathcal{I}[(v_{CO}=1,J',M',\Omega',v')\leftarrow(v_{CO}=0,J'',M'',\Omega'',v'')]$$
$$=\mathcal{N}(J'',M'',\Omega'',v'')\left|\sum_{j''n''}\sum_{j'n'}C^{J''\Omega''}_{v'',j''n''}C^{J'\Omega'}_{v',j'n'}\langle J'M'\Omega'j'|\varepsilon\cdot\mu|J''M''\Omega''j''\rangle\delta_{n'n''}\right|^2, \tag{A3}$$

where $\mathcal{N}(J'',M'',\Omega'',v'')$ is the Boltzmann factor $\exp(-E_{J''M''\Omega''v''}/kT)$ for the $(v_{CO}=0,J'',M'',\Omega'',v'')$ level. In the usual case where the complexes are not oriented, all M are equiprobable and the intensity for the $(v_{CO}=1,J',\Omega',v')\leftarrow(v_{CO}=0,J'',\Omega'',v'')$ transition is obtained by summing Eq. (A3) over M', M'',

$$\mathcal{I}[(v_{CO}=1,J',\Omega',v')\leftarrow(v_{CO}=0,J'',\Omega'',v'')]$$
$$=\frac{\varepsilon^2\mu_{CO}^2}{3}\mathcal{N}(J'',M'',\Omega'',v'')(2J''+1)(2J'+1)\begin{pmatrix}J' & 1 & J''\\ \Omega' & \Omega''-\Omega' & -\Omega''\end{pmatrix}^2$$
$$\times\left|\sum_{j''j'n}(2j''+1)(2j'+1)C^{J''\Omega''}_{v'',j''n}C^{J'\Omega'}_{v',j'n}\begin{pmatrix}j' & 1 & j''\\ 0 & 0 & 0\end{pmatrix}\begin{pmatrix}j' & 1 & j''\\ -\Omega' & \Omega'-\Omega'' & \Omega''\end{pmatrix}\right|^2. \tag{A4}$$

Note that considering only positive values of Ω implies multiplying intensities by 2 when Ω' or Ω'' is different from zero.

To get the microwave absorption spectrum, μ_{CO} has to be replaced by the permanent dipole moment of CO (it is a constant factor for the whole spectrum), the lines with "negative frequencies" (in our spectrum, where the origin is the $v_{CO}=1\leftarrow v_{CO}=0$ transition) have to be suppressed, the rest being identical. In particular, the bending excitation should be observable.

APPENDIX B: INERTIA TENSOR FOR Ar···CO CONSIDERED AS A RIGID BODY

In the (x',y',z') body-fixed frame where z' is parallel to **R** and x' lies in the molecular plane, such that the x' coordinate of **r** (going from C to O) is positive, the matrix of inertia is

$$\begin{pmatrix}I_{x'x'} & I_{x'y'} & I_{x'z'}\\ I_{y'x'} & I_{y'y'} & I_{y'z'}\\ I_{z'x'} & I_{z'y'} & I_{z'z'}\end{pmatrix}$$
$$=\begin{pmatrix}I_r\cos^2\theta+I_R & 0 & -I_r\sin\theta\cos\theta\\ 0 & I_r+I_R & 0\\ -I_r\sin\theta\cos\theta & 0 & I_r\sin^2\theta\end{pmatrix}, \tag{B1}$$

where $I_r=\mu r^2$ with $\mu=M_CM_O/(M_C+M_O)$ being the reduced mass of CO and r its bond distance, and $I_R=mR^2$ [with $m=M_{Ar}M_{CO}/(M_{Ar}+M_{CO})$]. By diagonalizing the inertia matrix in Eq. (B1), one obtains the moments of inertia

$$I_a=\frac{1}{2}[I_c-\sqrt{I_c^2-4I_r\sin^2\theta(2I_r\cos^2\theta+I_R)}]$$
$$=I_r\sin^2(\theta+\alpha)+I_R\sin^2\alpha,$$
$$I_b=\frac{1}{2}[I_c+\sqrt{I_c^2-4I_r\sin^2\theta(2I_r\cos^2\theta+I_R)}] \tag{B2}$$
$$=I_r\cos^2(\theta+\alpha)+I_R\cos^2\alpha,$$

from which the constants of inertia are readily obtained ($A=\hbar^2/2I_a$, etc...). In Eq. (B2), α is the angle by which to rotate the (x',y',z') frame about y' to get the inertia axes, given by

$$\alpha=\frac{1}{2}\arctan\left(\frac{-\rho\sin 2\theta}{1+\rho\cos 2\theta}\right), \tag{B3}$$

where $\rho=\mu r^2/mR^2$.

The rotational constants obtained for the two configurations chosen in this work (equilibrium and averaged) are presented in Table II. The masses were taken as $M_{Ar}=40$, $M_C=12$, and $M_O=16$ g mol^{-1}. r was deduced from the rotational constant of CO, $B_{CO}=\hbar^2/2\mu r^2$, with B_{CO} taken as B_e from Ref. 28 (=1.9313 cm^{-1}, which gives $r=1.1281$ Å). For the equilibrium geometry, Eq. (B3) gives $\alpha_e=0.334°$, hence $\theta_e+\alpha_e=100.334°$, and for the averaged geometry $\alpha_0=-0.898°$, hence $\theta_0+\alpha_0=51.4°$. Since I_R is about 20 times larger than I_r, α remains close to zero and $I_b\simeq I_c\simeq I_R$. On the other hand, I_A is much more sensitive to the value of θ, which explains the large difference between the two values of A in the two structures.

Downloaded 19 Aug 2003 to 128.125.187.57. Redistribution subject to AIP license or copyright, see http://ojps.aip.org/jcpo/jcpcr.jsp

[1] J. A. Beswick and J. Jortner, Adv. Chem. Phys. **47**, 363 (1981).
[2] *Structure and Dynamics of Weakly Bound Molecular Complexes*, edited by A. Weber (Reidel, Dordrecht, 1987).
[3] R. E. Miller, Science **240**, 447 (1988).
[4] K. C. Janda and C. R. Bieler, *Atomic and Molecular Clusters*, edited by E. R. Bernstein (Elsevier, New York/Amsterdam, 1990).
[5] D. J. Nesbitt, Chem. Rev. **88**, 843 (1988).
[6] J. M. Hutson, Annu. Rev. Phys. Chem. **41**, 123 (1990).
[7] *Dynamics of Polyatomic van der Waals Complexes*, Vol. 227 in NATO Advanced Study Institute, Series B: Physics, edited by N. Halberstadt and K. C. Janda (Plenum, New York, 1990).
[8] R. J. Le Roy and J. G. Carley, Adv. Chem. Phys. **42**, 353 (1980).
[9] G. Brocks and A. van der Avoird, in *Structure and Dynamics of Weakly Bound Molecular Complexes*, edited by A. Weber (Reidel, Dordrecht, 1987), pp. 337–355; G. Brocks (unpublished results).
[10] J. I. Cline, D. D. Evard, F. Thommen, and K. C. Janda, J. Chem. Phys. **84**, 1165 (1986); J. I. Cline, B. P. Reid, D. D. Evard, N. Sivakumar, N. Halberstadt, and K. C. Janda, *ibid.* **89**, 3535 (1988).
[11] D. W. Brinza, C. M. Western, D. D. Evard, F. Thommen, B. A. Swartz, and K. C. Janda, J. Phys. Chem. **88**, 2004 (1984); D. D. Evard, F. Thommen, and K. C. Janda, J. Chem. Phys. **84**, 3630 (1986); D. D. Evard, F. Thommen, J. I. Cline, and K. C. Janda, J. Phys. Chem. **91**, 2508 (1987); J. I. Cline, N. Sivakumar, D. D. Evard, C. R. Bieler, B. P. Reid, N. Halberstadt, S. R. Hair, and K. C. Janda, J. Chem. Phys. **90**, 2605 (1989).
[12] D. D. Evard, C. R. Bieler, J. I. Cline, N. Sivakumar, and K. C. Janda, J. Chem. Phys. **89**, 2829 (1988).
[13] C. R. Bieler, K. E. Spence, and K. C. Janda, J. Phys. Chem. **95**, 5058 (1991).
[14] J. M. Hutson, J. Chem. Phys. **89**, 4550 (1988); J. M. Hutson and B. J. Howard, Mol. Phys. **45**, 769 (1982); J. M. Hutson, J. Chem. Phys. **96**, 6752 (1992); J. M. Hutson, J. Phys. Chem. **96**, 4237 (1992); C. M. Lovejoy, J. M. Hutson, and D. J. Nesbitt, J. Chem. Phys. **97**, 8009 (1992).
[15] D. C. Clary and D. J. Nesbitt, J. Chem. Phys. **90**, 7000 (1989).
[16] A. R. W. McKellar, J. Chem. Phys. **93**, 18 (1990); Chem. Phys. Lett. **186**, 58 (1991); C. E. Chuaqui, R. J. Le Roy, and A. R. W. McKellar (to be published).
[17] G. A. Parker and R. T Pack, J. Chem. Phys. **69**, 3268 (1978).
[18] K. Mirsky, Chem. Phys. **46**, 445 (1980).
[19] C. A. Parish, J. D. Augspurger, and C. E. Dykstra, J. Phys. Chem. **96**, 2069 (1992); C. E. Dykstra, J. Am. Chem. Soc. **111**, 6168 (1989).
[20] S. K. Shin (to be published).
[21] A. De Piante, E. J. Campbell, and S. J. Buelow, Rev. Sci. Instrum. **60**, 852 (1989).
[22] A. R. W. McKellar, Y. P. Zeng, S. W. Sharpe, C. Wittig, and R. A. Beaudet, J. Mol. Spectrosc. **153**, 475 (1992).
[23] T. Ogata, W. Jäger, I. Ozier, and M. C. L. Gerry, J. Chem. Phys. **98**, 9399 (1993).
[24] M. Havenith, G. Hilpert, M. Petri, and W. Urban, Mol. Phys. **84**, 1003 (1994).
[25] J. Tennyson, S. Miller, and B. T. Sutcliffe, J. Chem. Soc. Faraday Trans. 2 **84**, 1295 (1988).
[26] D. J. Diestler, J. Chem. Phys. **60**, 2692 (1974).
[27] B. P. Reid, K. C. Janda, and N. Halberstadt, J. Phys. Chem. **92**, 587 (1988); J. I. Cline, B. P. Reid, D. D. Evard, N. Sivakumar, N. Halberstadt, and K. C. Janda, J. Chem. Phys. **89**, 3535 (1988).
[28] *Molecular Spectra and Molecular Structure*, edited by K. P. Huber and G. Herzberg (Van Nostrand Reinhold, Toronto, 1979), Vol. IV.
[29] D. J. Nesbitt and R. Naaman, J. Chem. Phys. **91**, 3801 (1989).
[30] O. Roncero, J. A. Beswick, N. Halberstadt, P. Villarreal, and G. Delgado-Barrio, J. Chem. Phys. **92**, 3348 (1990).
[31] A. Ernesti and J. M. Hutson (unpublished).
[32] W. Jäger and M. C. L. Gerry, Chem. Phys. Lett. **196**, 274 (1992).
[33] G. Henderson and G. E. Ewing, Mol. Phys. **27**, 903 (1973).
[34] A. R. W. McKellar, J. Chem. Phys. **88**, 4190 (1988).
[35] R. N. Zare, *Angular Momentum* (Wiley, New York, 1988).

Downloaded 19 Aug 2003 to 128.125.187.57. Redistribution subject to AIP license or copyright, see http://ojps.aip.org/jcpo/jcpcr.jsp